Computation of X-ray powder diffractograms of cement components and its application to phase analysis and hydration performance of OPC cement

ROHAN JADHAV and N C DEBNATH[*]

Department of Physics, Institute of Chemical Technology, Mumbai 400 019, India

Abstract. The importance of computed X-ray diffraction patterns of various polymorphs of alite (M_3, T_1, R), belite (β, γ), aluminate (cubic, orthorhombic), aluminoferrite, gypsum and hemihydrate in the quantitative phase analysis of cement and its early stage hydration performance is highlighted in this work with three OPC samples. The analysis shows that the predominant silicate phases present in all the samples are M_3-alite phase and β-belite phase, respectively. Both cubic and orthorhombic phases of C_3A, brownmillerite, gypsum and hemihydrates are present at different levels. Quantitative phase analysis of cement by Rietveld refinement method provides more accurate and comprehensive data of the phase composition compared to Bogue method. The comparative hydration performance of these samples was studied with w/c ratio, 0·5 and the results are interpreted in the light of difference in phase compositions viz. β-C_2S/C_3S ratio, fraction of finer cement particles present in the samples and theoretical modeling of C_3S hydration.

Keywords. Portland cement; X-ray diffraction; crystal structure; characterization; Rietveld method.

1. Introduction

Ordinary Portland cement and clinker are highly complex materials consisting of several crystalline phases. The four major components of OPC cement are alite (C_3S–Ca_3SiO_5), belite (C_2S–Ca_2SiO_4), aluminate (C_3A–$Ca_3Al_2O_6$), and aluminoferrite (C_4AF) while, the minor components are gypsum, calcium sulphate hemihydrate etc. Each of the major components, in turn, can exist in several polymorphic phases. Alite has seven polymorphic forms, belite can be in four polymorphic forms, aluminate exists in two crystal forms, aluminoferrite exists in orthorhombic phase and calcium sulphates can have more than one crystal phases (Hewlett 1988; Taylor 1997). A comprehensive analysis of commercial cement requires the identification of the specific mineralogical phases of all major and minor components that are present in cement and also their relative abundance. Since the hydraulic properties of cement depend quite substantially on the specific mineralogical phase and its relative abundance in cement, both qualitative and quantitative phase analyses of different mineralogical phases of the components of cement are very important to understand and predict the performance of cement and the resulting concrete.

There are several methods which may be used to determine the phase and phase composition of the cement. X-ray powder diffraction method is highly suitable for both qualitative and quantitative phase analyses of cement and clinker. The elemental composition of cement is usually determined by X-ray fluorescence method (XRF). In cement industry, the most common method that is used to estimate the mineralogical composition of cement clinker from elemental composition of cement is known as Bogue method (Bogue 1955; Hewlett 1988; American Standard ASTM C 150-94). This method is based on the assumption that each of the four major components (alite, belite, aluminate and ferrite) of cement clinker is a function of four oxide components viz. CaO, SiO_2, Al_2O_3 and Fe_2O_3. This method is used worldwide as a quality control method for OPC cements. One of the basic assumptions used in Bogue calculation is thermal equilibrium of the system at high temperature, which may not necessarily be correct and may be a source of error in quantitative analysis. Bogue method normally underestimates (C_3S + C_2S) content, overestimates the C_3A fraction and underestimates the C_4AF content (De La Torre et al 2002). The second method, quantitative phase analysis (QPA) of cement, is based on the analysis of X-ray powder diffraction patterns of cement with Rietveld refinement method (Rietveld 1969; Young et al 1977; Hill and Howard 1987; Bish and Howard 1988; Young 1993; De La Torre et al 2001; Costa and Marchi 2003; Scrivener et al 2004; Taylor and Hinezak 2004). Although Rietveld method does not require any internal standard like rutile or corundum, it requires the crystal structure of all the component phases to be known in advance, as the process consists of the comparison of the experimentally measured and theoretically calculated diffraction patterns of each component phase present in the cementitious material.

[*]Author for correspondence (ndebnath5@rediffmail.com)

One of the major problems encountered in the qualitative and quantitative analysis of cement is that there are strong overlapping of major diffraction peaks of all the main phases of cement components in the angular range of 2θ values from 30° to 35° (Cu K$_{\alpha1}$, λ = 1·540560 Å), making the identification of the individual components extremely difficult. Second major problem which adds to the complexity of the diffractograms of cement is that each individual component like alite, belite, aluminate, and aluminoferrite can crystallize in several polymorphic forms depending on their composition and this must be identified *a priori* before the analysis can be undertaken. In order to address this problem we have used theoretical techniques to generate a set of X-ray powder diffractograms of the important phases of each individual component of cement from the representative samples of stable polymorphic forms of these components and their crystal structure data. This method provides the unique diffraction pattern of each polymorphic form which might be used as a standard for comparison and also for analysis of the multiphase composite material like cement and cement clinker.

The primary objective of this work is to compute theoretically the X-ray powder diffraction patterns of different polymorphs of alite, belite, aluminate, aluminoferrite and other minor phases like gypsum, hemihydrate etc that are normally present in cement and utilize the computed profiles for both qualitative and quantitative phase analysis of different OPC cement samples and also for analysis of their hydration performance. From literature search, we have identified several stable polymorphs of the four major components and several minor phases of cement with slight variation in their chemical composition and crystal structure data and computed their diffraction patterns by using various unit cell parameters, space groups, fractional atomic positions, thermal parameters, site occupation numbers etc which are determined from the experimental X-ray diffraction study of single crystals of those compounds (Colville and Geller 1971; Mondal and Jeffery 1975; Nishi and Takéuchi 1975, 1984; Golovastikov *et al* 1975; Jost *et al* 1977; Okada and Ossaka 1980; Udagawa *et al* 1980; Benzou *et al* 1995; Mumme 1995; Schofield *et al* 1996; Peterson 2003; Inorganic Crystal Structure Database).

The computed diffraction profiles which are unique for each polymorph have been used to establish the identity of each component and its specific crystal phase in the multiphase cement system, since the various components present in cement diffract independently (Stutzman 1996). Secondly, the peaks that are free from overlap from other phases can also be identified and used for quantitative analysis of individual phase present in a mixture of cement and other components. Finally, we have used the Rietveld method to carry out quantitative phase analysis of all the samples and compare the results with the data calculated by Bogue method. The effect of the difference in phase compositions and particle size distributions of these samples in early stage of hydration performance is discussed in detail in the light of theoretical model for hydration of C$_3$S particles.

2. Experimental

Three commercial cement samples *S*1, *S*2 and *S*3 from different Indian manufacturers were used in this work for a comparative study of phase composition and hydration performance. Rutile sample Tiona-595 (Millennium Chemicals, Australia) was used in this work as an internal standard for measuring the degree of hydration of these samples by QXRD technique (Taylor 1997). In order to study the progress of cement hydration, cement paste samples were prepared with water to cement ratio of 0·5 and the hydration reaction was monitored for 6 h, 12 h, 18 h, 24 h and 3 days and the corresponding samples were prepared by first dipping each paste sample in acetone for 30 min and subsequently dipping in diethyl ether for another 30 min. The samples were then dried in an oven for 3 h at 105° C and ground to fine powder using mortar and pestle. The paste samples analysed by QXRD technique were prepared by homogeneously mixing dried cement paste powder and rutile in the weight ratio of 5:1 and the corresponding diffractograms were recorded for quantitative measurement of the degree of hydration (α). The progress of hydration reaction in cement paste was monitored by measuring the amount of unreacted C$_3$S component present in the paste as a function of hydration time.

The X-ray diffractograms of different samples were recorded on Panalytical X'Pert PRO X-ray diffractometer with Bragg–Brentano geometry. The wavelengths of X-rays used in this work for recording data were Cu K$_{\alpha}$ radiation, λ_1 = 1·540560 Å and λ_2 = 1·544390 Å with λ_2/λ_1 = 0·5. Powder samples were loaded on aluminum sample holder having dimensions $2 \times 1·5 \times 0·2$ cm (vol. 0·6 cm^3). The experimental conditions for data recording were as follows: X-ray tube was operated at 40 kV with 30 mA, fixed divergence slit with slit size 1·0°, step size of 0·017° with 5·1686 s/step. The data was collected for each sample over 2θ values ranging from 4° to 80°.

Similarly, XRF data of cement samples were generated on Philips PW2404 XRF spectrometer. The X-ray tube was operated at 60 kV with 50 mA. The diameter of the pellet used for XRF analysis was 37 mm and the pellet was prepared by mixing 4 g of sample with 1 g of microcrystalline methyl cellulose and by applying 15 T pressure for one min.

The particle size distribution (PSD) of OPC cement samples was determined by dispersing the cement samples in ethylene glycol medium with refractive index, 1·42857 and using HORIBA LA-300 set up. The real and imaginary part of refractive indices for cement particles were taken as $n_{\text{real}} = 1·7$ and $n_{\text{k}} = 0·1$, respectively for computing particle size distribution data (Ferraris *et al* 2004).

3. Theoretical

3.1 *X-ray powder diffraction*

X-ray powder diffractogram of a crystalline material provides a unique diffraction pattern of each material when

monochromatic X-rays of a given wavelength, λ, is scattered from the material over a wide range of 2θ values. The powder diffractogram consists of a series of diffraction peaks each of which is characterized by its position (2θ), intensity (I) and Miller indices (hkl) of the set of crystal planes contributing to a particular peak. The characteristic features of the diffractogram can be calculated by using inputs like unit cell parameters ($a, b, c, \alpha, \beta, \gamma$), space group, fractional position of the atoms in the unit cell, site occupation number and thermal parameters etc. The intensity of the diffraction peak is given by following equation:

$$I_{cal} = |F_{hkl}|^2 \, p \left(\frac{1 + \cos^2 2\theta}{\sin^2 \theta \cos \theta} \right) e^{-2M}. \quad (1)$$

All the parameters are as defined in the text of Cullity (1978).

3.2 *Rietveld refinement method*

Rietveld refinement method (Rietveld 1969; Young *et al* 1977; Hill and Howard 1987; Bish and Howard 1988; Young 1993; De La Torre *et al* 2001; Costa and Marchi 2003; Scrivener *et al* 2004; Taylor and Hinezak 2004) is a very useful method to analyse X-ray diffraction (XRD) data of complex materials. The method fits to a multivariable structure-background-profile model to the experimental XRD data of the material under investigation. In this method, user defined parameters are optimized using least-square procedure to minimize the difference between the observed (experimental) and calculated diffraction patterns based on approximate crystal structure and instrumental parameters. The scale factor of the phases present in the sample is used to calculate the phase composition of the material (Hill and Howard 1987; Bish and Howard 1988).

The key equations which are used in the implementation of Rietveld method in practice are described below:

The full "multiphase" Rietveld expression for the intensity y_i at a point i of the step scan is (Young 1993):

$$y_{ci} = \left[\sum_j S_j \sum_{hkl_j} L_{hkl_j} \left| F_{hkl_j} \right|^2 \phi(2\theta_i - 2\theta_{hkl_j}) \, P_{hkl_j} \, A \right] + y_{bi}, \quad (2)$$

where y_{ci} is the calculated intensity at point i, y_{bi} the background contribution to intensity at point i, S_j the scale factor of phase j, hkl the Miller indices hkl for a Bragg reflection of phase j, L_{hkl} the Lorentz polarization and multiplicity factors, F_{hkl} the structure factor for Bragg reflection hkl, P_{hkl} the preferred orientation function, A the absorption factor and ϕ the peak profile function.

The quantity which is minimized in the refinement process is residual S'_y

$$S'_y = \sum_i w_i (y_{oi} - y_{ci})^2, \quad (3)$$

where, w_i is the $1/y_{oi}$, y_{oi} the observed intensity at a point i, y_{ci} the calculated intensity at a point i.

In practice, the different 'R' factors like R_p, R_{wp}, R_{exp} and 'χ'(R_{wp}/R_{exp}) are used to estimate the goodness of fit (Young 1993; Rodríguez-Carvajal, Fullprof 2000).

3.2a *Quantitative phase analysis*:

The quantitative phase analysis in Rietveld method relies on the following relationship (Hill and Howard 1987; Bish and Howard 1988).

$$W_p = S_p(ZMV)_p / \sum_{i=1}^n S_i(ZMV)_i, \quad (4)$$

where W_p is the relative weight fraction of phase p in a mixture of n phases, S, Z, M and V are Rietveld scale factor, number of formula units per unit cell, mass of the formula unit (in atomic mass units) and volume of the unit cell, respectively.

3.3 *Mathematical modeling of hydration of tricalcium silicate (C_3S) particles*

In order to understand the hydration process of OPC cement particles we have studied theoretically the hydration of spherical C_3S particles as C_3S is the major component of OPC cement. The C_3S hydration model used in this work was developed by Pommersheim and Clifton (1979, 1982). In this model it is assumed that the hydrating particles remain isothermal during the hydration process and their hydration rates do not depend upon their positions in the system. These particles are considered to be uniform in size and spherical in shape. The hydration products that formed around the particles are also assumed to have spherical symmetry. Two distinct calcium silicate hydrate layers are formed around the hydrating particles, an inner hydrate layer which grows inward from the original boundary (radius R) of the C_3S particle and outer layer which grows outward in the pore solution.

Application of appropriate boundary and interface conditions to diffusion of chemical species through these hydrate layers yields the following differential equation:

$$-\frac{dt}{\tau} = \left[\left(\frac{1}{my^2} + \frac{1}{y} - 1 \right) + \frac{D_i}{D_x} \frac{x}{R} + \frac{D_i}{D_o} \left(1 - \frac{R}{r_o} \right) \right] y^2 dy, \quad (5)$$

where τ is the characteristic time defined as $aR^2\rho/C_o D_i$ and y the reduced radius, r_i/R, a the number of moles of water reacted per mole of C_3S consumed, ρ the molar density of C_3S particle, R the original radius of the particle, r_i and r_o are the inner and outer radii of the hydrating C_3S particle, D_i, D_x and D_o are the diffusivities through inner, middle and outer hydrate layer, respectively, m the reaction-diffusion modulus given by kR/D_i and k the first order surface rate constant for the reaction between C_3S and water.

The solution of the above differential equation with initial condition $y = 1$ at $t = 0$, predicts the radius of the unhydrated C_3S core (r_i) and the degree of hydration (α) as a function of time. α is given by following equation:

$$\alpha = 1 - y^3. \tag{6}$$

4. Computational procedure

4.1 *Computation of X-ray powder diffraction profiles of cement components and quantitative phase analysis of OPC cement using Rietveld refinement method*

The crystallographic software '*Fullprof* 2000' (Rodríguez-Carvajal, Fullprof 2000) was used in this study to compute the theoretical X-ray diffraction patterns of polymorphs of the different components that are generally present in OPC cement. X-ray CuK$_{\alpha 1}$ wavelength (1·540560 Å) was used in the computation of the X-ray diffraction patterns. The unit cell parameters (a, b, c, α, β and γ), space group and crystallographic phases of different compounds of different components of interest are listed in table 1. The other input parameters required for computation of diffraction patterns like fractional atomic position of the atoms in the unit cell, site occupation number and thermal displacement parameters etc of individual phases are available in references cited in table 1. As "Fullprof" accepts anisotropic thermal displacement parameter only in β form, other forms of this parameter like U's and B's in different literature have to be converted first to β form before computation of X-ray diffraction pattern. Later, Rietveld refinement process was carried out using the same software for quantitative phase analysis of OPC cement samples.

For quantitative phase analysis of X-ray diffractograms of OPC cement samples, we have included seven phases viz. M_3-alite (Mumme 1995), β-C$_2$S, both cubic and orthorhombic (Nishi and Takeuchi 1975) C$_3$A and brownmillerite along with minor phases like gypsum and calcium sulphate hemihydrate in the Rietveld refinement process. The backgrounds of the patterns were fitted with six-coefficient polynomial background function. The pseudo-Voigt function (pV) was used to fit the diffraction peaks of all included phases. The modified March's function was used to account for strong preferred orientation exhibited by gypsum phase.

Table 1. Crystallographic data for crystalline phases present in cement and clinker.

No.	Chemical composition	Phase	Space group	a (Å)	b (Å)	c (Å)	α	β	γ	Reference
					Major phases					
	Alite									
1.	Ca$_{2.99}$ Na$_{0.01}$ (Si$_{0.90}$ Al$_{0.04}$ Fe$_{0.02}$ P$_{0.03}$ Mg$_{0.05}$) O$_5$	Monoclinic M_3	Cm	12·235	7·073	9·298	90·0	116·3	90·0	(Mumme 1995; Peterson 2003)
2.	Ca$_3$(SiO$_4$)O	Triclinic T_1	$P-1$	11·67	14·24	13·72	105·5	94·3	90·0	(Golovastikov *et al* 1975; Peterson 2003)
3.	Ca$_{2.98}$Si$_{0.98}$ Al$_{0.04}$O$_5$	Rhombohedral R	$R\,3\,m$	7·135	7·135	25·586	90·0	90·0	120·0	(Nishi and Takeuchi 1984)
	Belite									
4.	β-Ca$_2$SiO$_4$	Monoclinic	$P\,21/n$	5·502	6·745	9·297	90·0	94·59	90·0	(Jost *et al* 1977)
5.	γ-Ca$_2$SiO$_4$	Orthorhombic	$Pbnm$	5·081	11·224	6·778	90·0	90·0	90·0	(Udagawa *et al* 1980)
	Tricalcium aluminate									
6.	Ca$_3$Al$_2$O$_6$	Cubic	$Pa3$	15·263	15·263	15·263	90·0	90·0	90·0	(Mondal and Jeffery 1975)
7.	Ca$_{8.5}$NaAl$_6$O$_{18}$	Orthorhombic	$Pbca$	10·868	10·856	15·128	90·0	90·0	90·0	(Nishi and Takeuchi 1975; Peterson 2003)
	Calcium aluminoferrite									
8.	Brownmillerite (Ca$_2$FeAlO$_5$)	Orthorhombic	$Ibm2$	5·584	14·60	5·374	90·0	90·0	90·0	(Colville and Geller 1971)
					Minor phases					
	Calcium sulphates									
9.	Gypsum: calcium sulphate dihydrate (CaSO$_4$·2H$_2$O)	Monoclinic	$I2/c$	5·6740	15·1049	6·4909	90·0	118·513	90·0	(Schofield *et al* 1996)
10.	Calcium sulphate hemihydrate (CaSO$_4$·0·5H$_2$O)	Monoclinic	$I1\,2\,1$	12·0344	6·9294	12·6757	90·0	90·265	90·0	(Benzou *et al* 1995)
	Tripotassium sodium disulphate									
11.	K$_3$Na(SO$_4$)$_2$	Trigonal	$P-3\,m$	5·6801	5·6801	7·309	90·0	90·0	120·0	(Okada and Ossaka 1980)

The most important parameters of refinement process viz. scale factors of all the phases, were refined simultaneously in the first stage itself and kept variable during the subsequent stages of refinement process. The zero point shift and polynomial background coefficients were refined respectively after the first step. In the next step, unit cell parameters a, b, c, α, β and γ were refined. During the refinement, the phases were given priorities as per their general weight percentage and also their scattering power (mass absorption coefficient, μ/ρ). Peak width parameter 'W' was also refined for all the phases in the same sequence.

In the second stage of the refinement process, fractional atomic positions for heavier atoms like Ca and Si are refined only for two major phases viz. alite and belite. The occupation number was refined for all the atoms of both the phases. The parameters for the preferred orientation of the gypsum

phase were refined first and then the refinement of the asymmetric peak shape parameters for the alite and belite was carried out. Finally peak shape parameters viz. U, V and η of pseudo-Voigt function were refined.

4.2 *Computation of mass percentage of components from XRF data of cement composition*

At the first stage of analysis, Bogue method (Bogue 1955; Hewlett 1988; American Standard ASTM C 150-94) was used to calculate the approximate mineralogical composition of the OPC cement samples from the elemental composition of the samples which were determined by XRF method. The formulae (Hewlett 1988) used for calculation of mass percentage of four major phases viz. C_3S, C_2S, C_3A
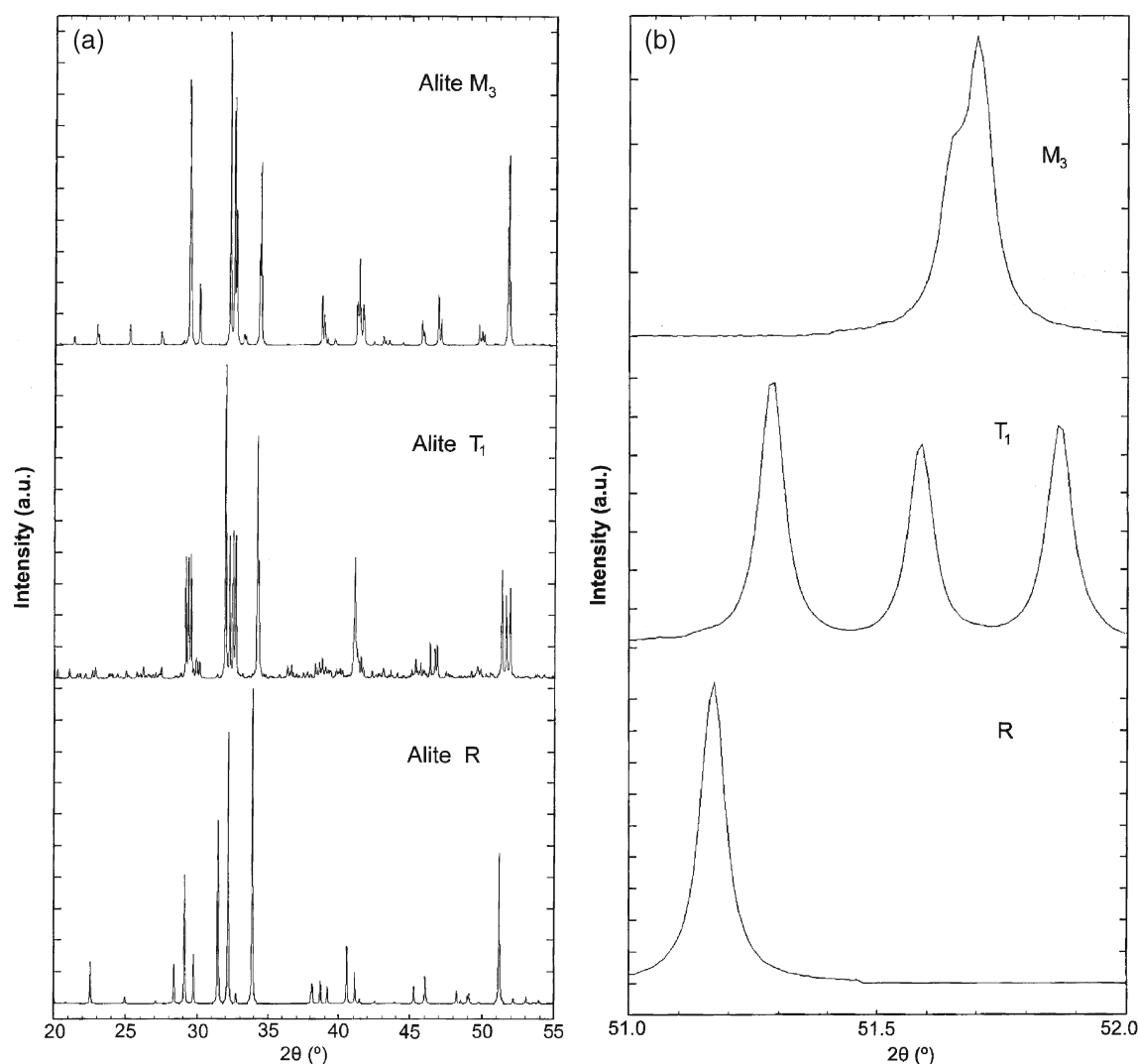

Figure 1. **a**. Computed diffractograms of alite polymorphs: monoclinic (M_3), triclinic (T_1) and rhombohedral (R) and **b**. alite peaks around $2\theta = 51°$–$52°$ of computed diffractograms of monoclinic (M_3), triclinic (T_1) and rhombohedral (R).

and C$_4$AF of cement samples are given below (American Standard ASTM C 150-94).

C = %CaO, S = %SiO$_2$, A = %Al$_2$O$_3$,

F = %Fe$_2$O$_3$, Ŝ = %SO$_3$,

$$C_3S = 4 \cdot 071 \times C - 7 \cdot 600 \times S - 6 \cdot 718 \times A$$
$$- 1 \cdot 430 \times F - 2 \cdot 857 \times \hat{S}, \tag{7}$$

$$C_2S = 2 \cdot 867 \times S - 0 \cdot 754 \times C_3S, \tag{8}$$

$$C_3A = 2 \cdot 65 \times A - 1 \cdot 692 \times F, \tag{9}$$

$$C_4AF = 3 \cdot 043 \times F, \tag{10}$$

where the %CaO, %SiO$_2$ etc are the mass percentage of the component oxides.

5. Results and discussion

The input data required for computation of X-ray powder diffractograms of different component phases of cement and clinker are provided in table 1 where the crystal structure data of 11 samples of alite, belite, aluminate, ferrite, gypsum, calcium sulphate hemihydrate and tripotassium sodium disulphate along with their chemical composition, type of crystal structures, space group and unit cell parameters etc are summarized. The other set of input data required for computation of diffraction pattern are fractional atomic position, site occupation number and thermal displacement parameters. These data for each phase are taken from the corresponding references cited in the last column of table 1.

The computed diffractograms of each individual phase of each component of cement and clinker are presented in graphical form (2θ vs I) in figures 1–6.

5.1 *Characteristic and distinguishing features of different cement components*

To facilitate the discussion of polymorphs of each component phase, we have presented the results in comparative figures. For example, figure 1a shows the computed diffractograms of three polymorphs of alite phases viz. monoclinic (M_3), triclinic (T_1) and rhombohedral (R) computed over 2θ angle varying from 20° to 55° for comparison among these polymorphs and also with experimental X-ray diffractograms of OPC cement samples. The unique distinguishing diffraction peaks of these polymorphs of alite are shown in figure 1b. The M_3 phase of alite shows a doublet at $2\theta = 51 \cdot 7°$ whereas

T_1 phase of alite shows a triplet at 51°–52° and rhombohedral R phase shows strong singlet at 51·16°. The diffraction pattern computed from monoclinic structure given by Mumme (Mumme 1995; Peterson 2003) shows a shoulder and a peak at $2\theta = 51 \cdot 7°$ instead of well resolved doublet as observed in the case of pure M_3 phase given by Nishi (Taylor 1997) which, however, is not computed here. This difference in the distinguishing features can be attributed to difference in the chemical composition of the two alite phases. The relatively lower Mg content (0·05%) (atomic percentage) in alite M_3 (Mumme 1995) is responsible for this average structure compared to that of pure alite M_3 phase given by Nishi which has about 0·11% MgO (Taylor 1997). The pure M_1 phase of alite, which is not computed here,
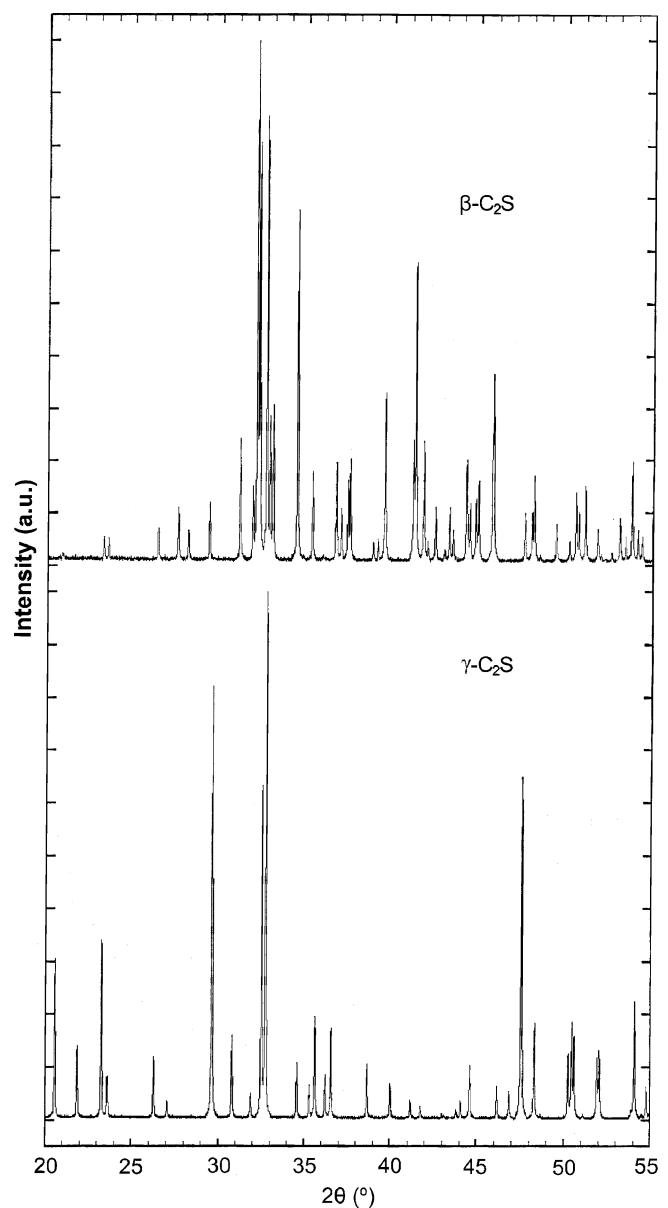

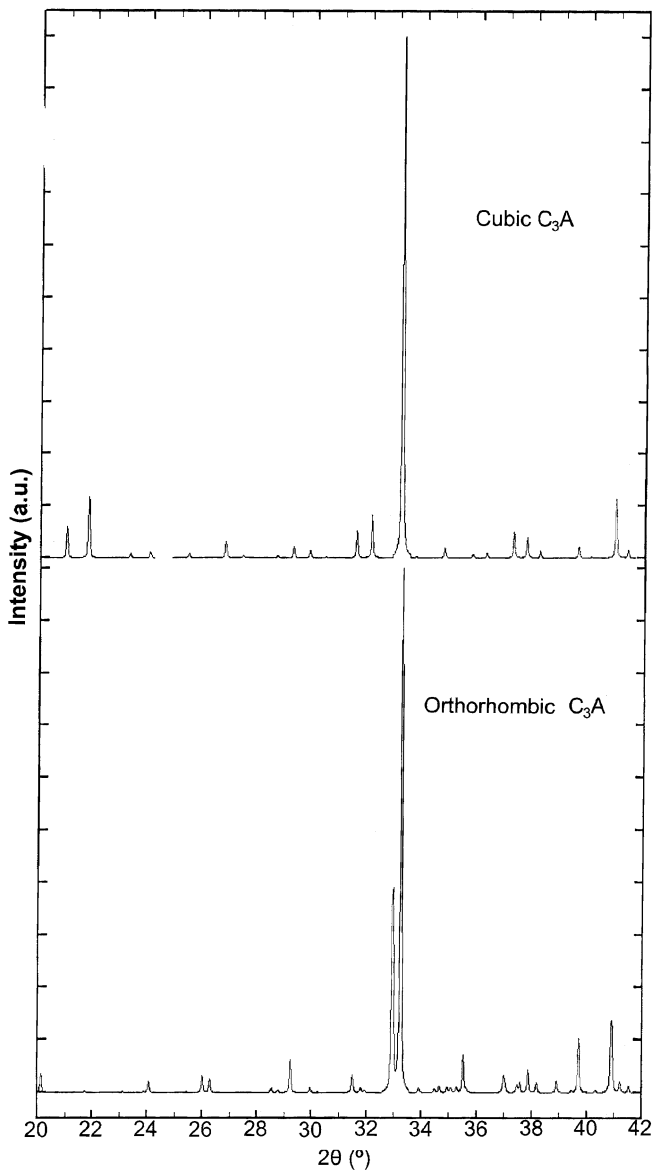**Figure 2.** Computed diffractograms of belite polymorphs: β-C$_2$S and γ-C$_2$S.

Figure 3. Computed diffractograms of tricalcium aluminate polymorphs: cubic and orthorhombic C_3A.

Figure 4. Computed diffractograms of brownmillerite (C_4AF).
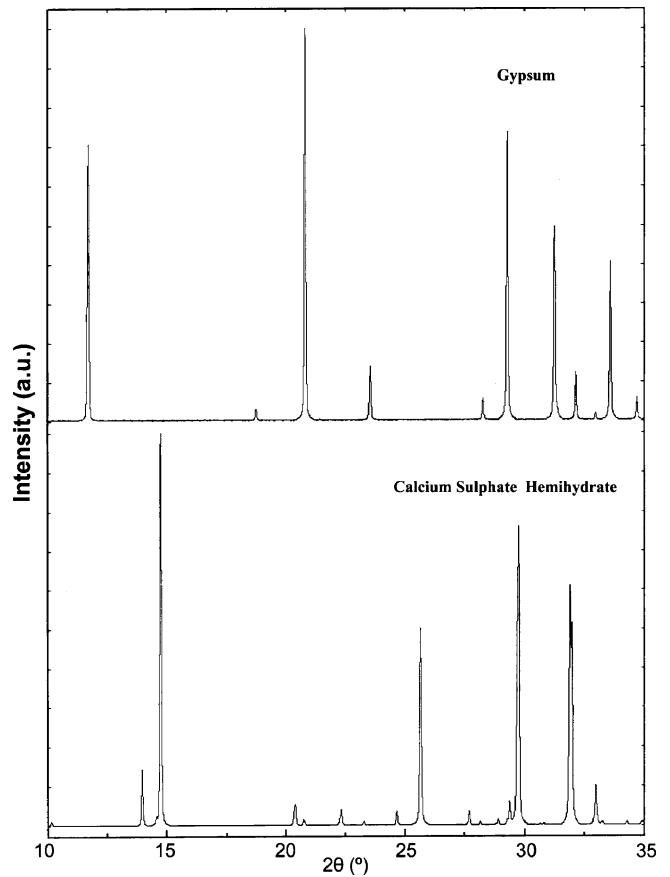
Figure 5. Computed diffractograms of gypsum and calcium sulphate hemihydrate.

shows a well defined singlet at $2\theta = 51 \cdot 7°$ (Taylor 1997). Figure 2 shows comparative diffractograms of two important belite phases viz. β-C_2S and γ-C_2S, computed in the range of 2θ values from 20° to 55°. For β-C_2S all the major peaks overlap with the M_3 phase of alite with the exception of distinct peaks at 2θ values of $31 \cdot 10°$ and $35 \cdot 29°$ which may be used for quantitative analysis of that phase in cement, if the intensity is clearly measurable in actual cement. γ-C_2S phase can be differentiated from β-C_2S phase by the unique distinguishing peak at $2\theta = 29 \cdot 63°$, $47 \cdot 53°$. It should be noted that γ-C_2S phase has inferior hydraulic property and therefore, this phase is undesirable in cement clinker at the cost of β-C_2S phase (Udagawa *et al* 1980; Stutzman 1996).

Figure 3 shows comparative diffractograms of cubic and orthorhombic tricalcium aluminate phase. The cubic phase
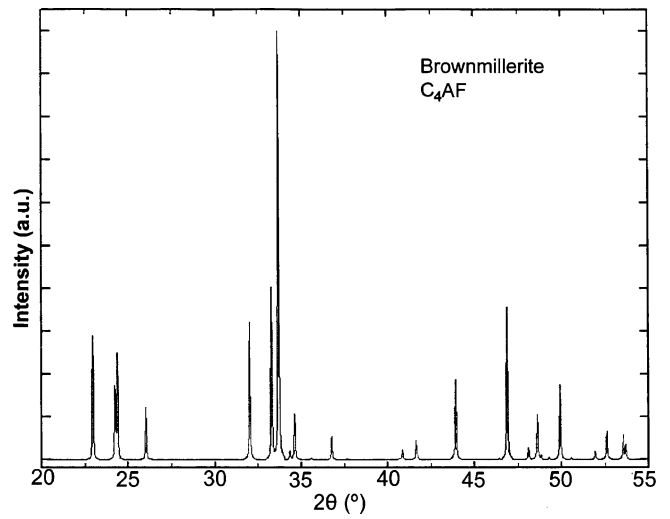
of C_3A is characterized by a strong peak at $33 \cdot 17°$ which falls in the overlap zone of the OPC cement ($2\theta = 30°$ to 35°). The orthorhombic phase of C_3A can be differentiated from the cubic phase of C_3A by the presence of a doublet with peak position at $32 \cdot 95°$ and $33 \cdot 23°$ in place of strong

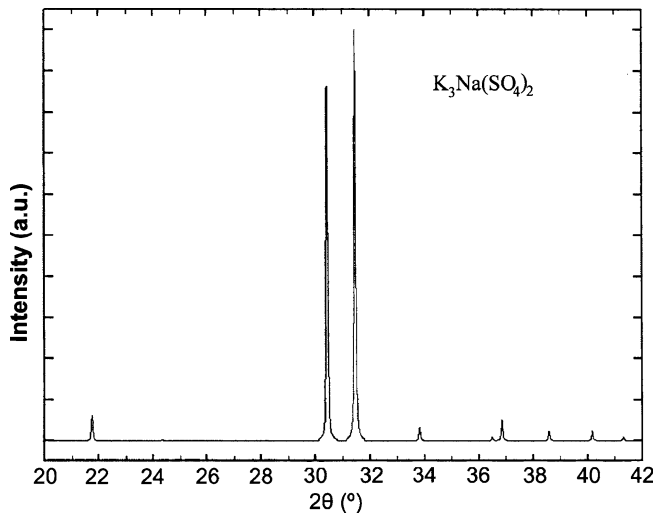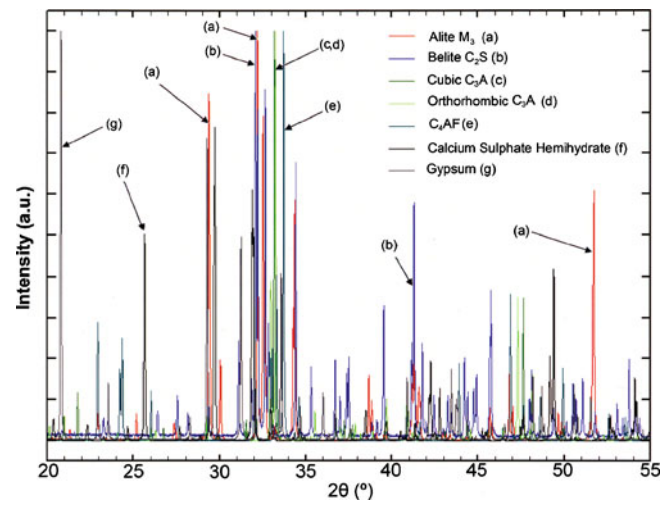**Figure 6.** Computed diffractograms of tripotassium sodium disulphate, $K_3Na(SO_4)_2$.

Figure 7. Superposition of X-ray diffractograms of alite M_3, belite β-C_2S, cubic and orthorhombic C_3A, brownmillerite C_4AF, gypsum and calcium sulphate hemihydrate.

Table 2. Distinguishing features of computed diffractograms of different components present in cementitious materials.

Phase	Polymorphs	P.D.F. card no.	Distinct features of diffractograms
Alite (C_3S)	Monoclinic M_3	42–551	Strong peak with a shoulder at $51 \cdot 7°$
	Triclinic T_1	31–301	Triplet between 51–$52°$ ($51 \cdot 3°$, $51 \cdot 58°$ and $51 \cdot 85°$)
	Rhombohedral, R	16–406	Strong singlet at $51 \cdot 16°$
	For M_3 phase, major peaks at $29 \cdot 35°$ and $51 \cdot 7°$ are essentially free from overlap and may be used for identification and quantitative analysis		
Belite (C_2S)	β-C_2S	33–302	Strong peaks at $32 \cdot 05°$, $32 \cdot 61°$ $34 \cdot 40°$ and $41 \cdot 28°$
	Peak at $31 \cdot 10°$ and $35 \cdot 30°$ are weak, but essentially free from overlap and can be used for quantitative analysis		
	γ-C_2S	31–297	Strong peaks at $32 \cdot 72°$, $29 \cdot 63°$ and $47 \cdot 53°$
Tricalcium aluminate (C_3A)	Cubic	38–1429	Strong peak at $33 \cdot 17°$ may be used for identification
	Peak at $28 \cdot 61$ is weak, but free from overlap and may be used for quantitative analysis		
	Orthorhombic	32–150	Two peaks at $32 \cdot 95°$ and $33 \cdot 23°$ are observed in place of single peak at $33 \cdot 17°$ as observed in cubic case
	Major peaks $33 \cdot 23°$ is in the region of overlap and difficult to use for quantitative purpose		
Calcium aluminoferrite ($Ca_2(Fe_x Al_{1-x})_2O_5$)	C_4AF-Ca_2FeAlO_5 (Brownmillerite)	30–226	Key diffraction peaks at $12 \cdot 1°$, $24 \cdot 4°$ and $33 \cdot 7°$
	For quantitative analysis suitable peaks at $12 \cdot 1°$, $24 \cdot 4°$ can be used		
Calcium sulphate dihydrate (Gypsum)	$CaSO_4 \cdot 2H_2O$	33–311	Key diffraction peaks which can be used for identification and quantitative analysis are $11 \cdot 71°$, $20 \cdot 80°$
Calcium sulphate hemihydrate ($CaSO_4 \cdot 0 \cdot 5H_2O$)	$CaSO_4 \cdot 0 \cdot 5H_2O$	41–224	Key diffraction peak at $14 \cdot 73°$ can be used for identification and quantitative analysis
Tripotassium sodium disulphate	$K_3Na(SO_4)_2$	20–926	Distinct doublet observed at $30 \cdot 45°$ and $31 \cdot 47°$

single peak at 33·17° as observed for cubic case. It may be noted that the incorporation of Na_2O in cubic C_3A beyond 1% causes the transformation of cubic phase to orthorhombic C_3A phase (Taylor 1997). However, it is difficult to identify individual aluminate phases in actual cement diffractograms. For "Brownmillerite (C_4AF)" phase of aluminoferrite (figure 4), the key differentiating peaks are located at 12·10°, 24·4° and 33·7° and the first two peaks may be used for quantitative analysis as the peak at 33·7° falls in the overlap zone.

The comparative diffractograms of gypsum and calcium sulphate hemihydrate are shown in figure 5. Gypsum phase in cement can be identified by the distinguishing peaks at

11·71° and 20·80°. Similarly, the hemihydrate phase can be identified by a strong distinguishing peak at 14·73°. The other minor phase, tripotassium sodium disulphate (figure 6) which shows a distinct doublet at 30·45° and 31·47° may be identified by these peaks. But it is difficult to identify this phase in cement because the angular position of the doublet falls in the overlap zone.

The key distinguishing features of each phase is summarized in table 2. The computed data of all the compounds have been compared with X-ray powder diffraction data file to validate the computed results (Stutzman 1996).

5.2 *Qualitative analysis of cement samples*

In order to compare the computed diffraction data of individual component phases and also to analyse the experimental X-ray powder diffractogram of OPC cement, we have superposed the calculated diffraction patterns of seven component phases viz. M_3 phase of alite, β phase of belite, both cubic and orthorhombic phases of aluminate, brownmillerite phase (C_4AF) of aluminoferrite, gypsum and calcium sulphate hemihydrate in the angular range of 2θ values of 20° to 55° as shown in figure 7. Different colour codes are used in figure 7 to differentiate the different components. In this superposed figure, all phases are normalized to 100% so that the extent of overlap of individual phase in a peak can be computed easily. When figure 7 is compared with the experimental diffractograms of cement samples $S1$, $S2$ and $S3$ (figure 8), several key features become quite obvious.

It is quite evident from figure 7, that the strongest Bragg's peaks of most of the component phases overlap strongly with each other in the angular range of 30° to 35°, making it very difficult to use this important part of the OPC cement diffractogram for identification of the phases present in cement. The monoclinic M_3 phase of "alite" has a major characteristic peak at $2\theta = 29·35°$ which is essentially free from overlap of β-C_2S phase and hence this peak may be used for quantitative analysis of "M_3 alite" phase in cement and in cement hydration products and also to determine the degree of hydration of cement when an internal standard is used with cement reaction products. The β-C_2S phase has a medium strong

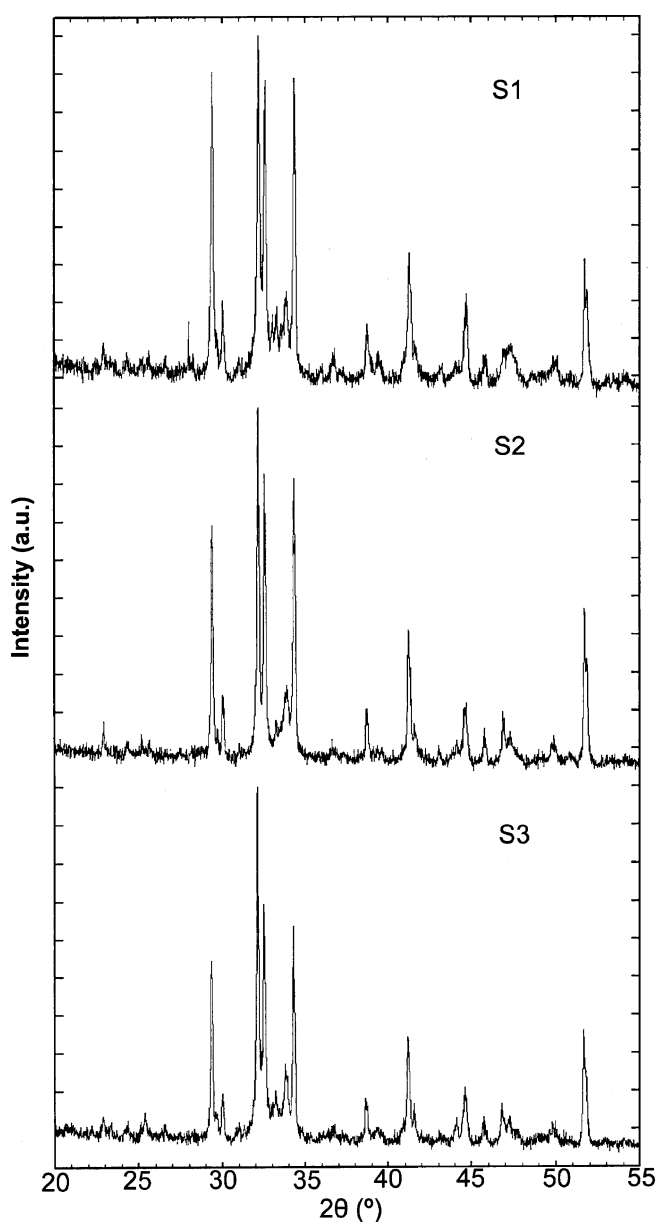**Figure 8.** Experimental X-ray diffractograms of OPC cement samples $S1$, $S2$ and $S3$.

Table 3. Elemental composition of OPC cement samples by X-ray fluorescence spectroscopy.

Oxides	OPC cement		
	$S1$	$S2$	$S3$
CaO	64·40	66·47	63·98
SiO_2	21·25	21·20	21·34
Al_2O_3	5·35	5·31	5·34
Fe_2O_3	4·00	4·11	4·68
K_2O	0·35	0·37	0·29
MgO	1·27	0·94	0·88
Na_2O	0·39	0·10	0·18
SO_3	1·54	1·69	2·45

peak at 41·28° which although has some overlap with alite phase, may also be explored for quantitative analysis as the % of contribution of β-C_2S and C_3S to this peak are roughly 62% and 28%, respectively. Since all the major peaks of C_4AF, cubic and orthorhombic C_3A lie in the range 30° to 35°, it is very difficult to identify these phases separately in cement. The striking similarity of M_3 alite phase (figure 1a) with OPC cement samples (figure 8) clearly indicates that the alite phase that is present in cement samples $S1$, $S2$ and $S3$ is monoclinic M_3 alite phase. The pure C_3S phase, which is the triclinic 'T_1' phase and the rhombohedral 'R' phase of alite are essentially absent in all the samples analysed in this study. The strong similarity of the peak at 41·28° of β-C_2S and the cement samples indicates that the belite phase present in all the samples is β-C_2S phase. The absence of strong characteristic peaks of γ phase of belite indicates that this phase is essentially absent in all the samples. The strong

peaks of all the four major components overlap strongly in the 2θ region of 31°–35° leading to 4 major peaks in OPC cement as shown in figure 8. However, this region is difficult to resolve and therefore, is less useful for analysis of cement components.

5.3 *Quantitative analysis of cement samples*

5.3a *Bogue method*: In the first stage of the quantitative phase analysis of three OPC cement samples, the mass percentages of four major components have been computed by Bogue formulae from the elemental composition of the samples which was determined by XRF spectroscopy (table 3). The results are summarized in table 4 along with the phase composition data computed from Rietveld analysis of X-ray diffractograms of the samples.

Table 4. Comparison of phase composition data of OPC cement samples by Rietveld refinement and Bogue methods.

| Phases		S1 Rietveld	S1 Bogue	S2 Rietveld	S2 Bogue	S3 Rietveld	S3 Bogue
Alite		58·31	54·64	59·97	63·14	50·12	48·72
Belite		19·65	19·70	19·29	13·16	21·41	24·43
C_3A (Ortho)		4·22	7·40	0·76	7·11	7·67	6·23
C_3A (Cubic)		3·54		9·31		9·60	
C_4AF (Brownmillerite)		8·64	12·17	8·71	12·51	6·31	14·24
Gypsum		1·17	—	0·0	—	1·27	—
Hemihydrate		4·48	—	1·97	—	3·62	—
Total		100·0	93·91	100·0	95·92	100·0	93·62
L. S. refinement factors	R_p	8·77		9·41		8·96	
	R_{wp}	11·3		12·0		11·3	
	R_{exp}	8·39		9·14		8·38	
	χ^2	1·81		1·93		1·83	
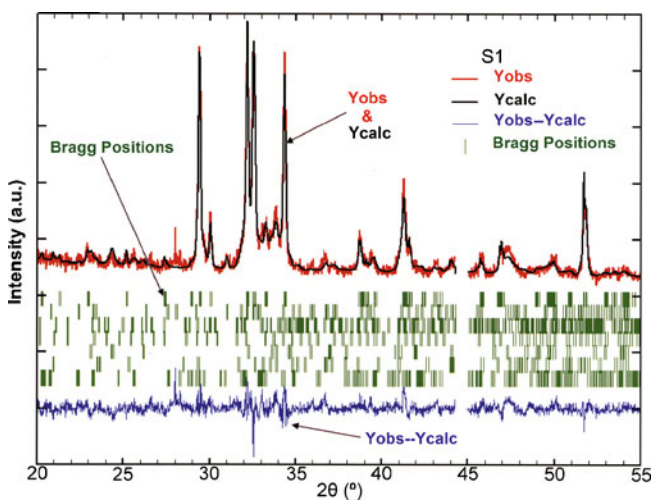
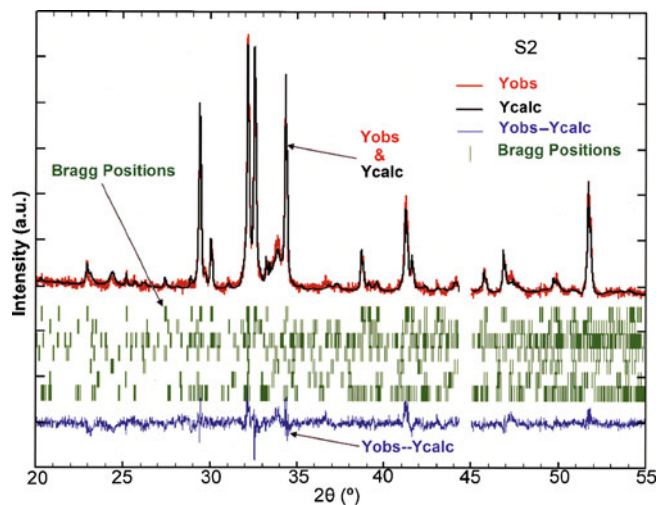**Figure 9.** Rietveld refinement of OPC cement sample $S1$.

Figure 10. Rietveld refinement of OPC cement sample $S2$.

The percentage of C_3S component is lowest in sample $S3$ (48·72%), highest in sample $S2$ (63·14%) and intermediate in sample $S1$ (54·64%). This difference in C_3S percentage is quite significant and is likely to affect the hydraulic properties of each sample during hydration process. On the other hand, C_2S content is the highest in sample $S3$ (24·43%), lowest in sample $S2$ (13·16%) and intermediate in sample $S1$ (19·70%). Although there is substantial variation in the relative proportion of C_3S and C_2S in different samples, the sum of C_3S and C_2S percentage comes quite close to each other (72–76%). C_3A contents of samples $S1$ and $S2$ are approximately same, 7·40% and 7·11%, respectively but lower in $S3$ which is 6·23%. Percentage of C_4AF is quite

similar in samples $S1$ and $S2$, 12·17% and 12·51%, respectively but slightly higher in sample $S3$, 14·24%. Bogue calculation did not account for 4–6% of material present in the samples. This difference may be attributed to 4–5% of gypsum, hemihydrate and other minor phases present in cement samples.

5.3b *Rietveld refinement method*:   In the second stage of quantitative phase analysis of the samples, Rietveld refinement method has been used for more accurate calculations of the phase composition of OPC cement. The calculated diffractogram (black), observed diffractogram (red), difference pattern (blue) and Bragg's positions (green) of the cement samples are shown in figures 9, 10 and 11 for the samples $S1$, $S2$ and $S3$, respectively.

The phase composition of the cement samples obtained at the end of refinement process and the least square R-factors like R_p, R_{wp}, R_{exp} and χ^2 are shown in table 4. The R_p, R_{wp} and R_{exp} values of the samples are in the range of 8–9, 11–12 and 8–9, respectively. The χ^2 values obtained for samples $S1$, $S2$ and $S3$ are 1·81, 1·93 and 1·83, respectively. For complex materials like cement, these values indicate quite a good fitting of the diffractograms as confirmed by literature data (Taylor and Hinezak 2004).

The alite content of the samples $S1$ (58·31%) and $S2$ (59·97%) is quite close to each other, but the alite content of the sample $S3$ is much lower, which is only 50·12%. Similarly the belite content is essentially same in $S1$ and $S2$ viz. 19·65% and 19·29%, respectively but is slightly higher for $S3$ sample (21·41%). This indicates a marked improvement of mass percentage of alite and belite phases present in these samples compared with the values obtained by Bogue method as discussed in previous section. Both cubic
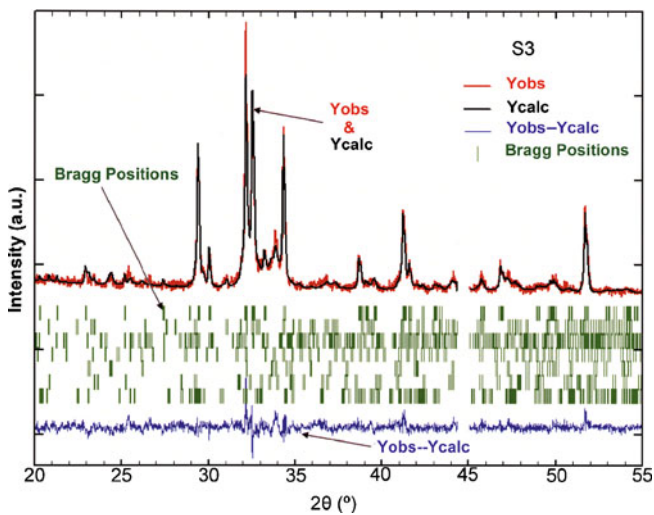

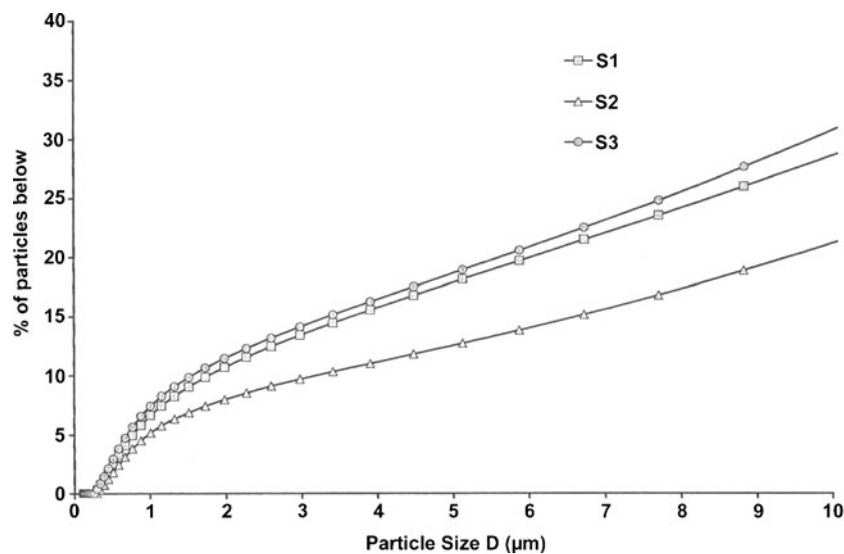**Figure 11.**   Rietveld refinement of OPC cement sample $S3$.

Figure 12.   Cumulative particle size distribution (0–10 μm) of OPC cement samples $S1$, $S2$ and $S3$.

and orthorhombic phases of tricalcium aluminate (C_3A) are present in $S1$ and $S3$ samples. In contrast, C_3A content of $S2$ sample is dominated by cubic phase (cubic 9·31% with orthorhombic only 0·76%). The total C_3A content of $S3$ is much higher, 17·27%, in contrast with the other two samples, $S1$ and $S2$ where C_3A content is in the range of 8–9%. The C_4AF content of $S1$ (8·64%) and $S2$ (8·71%) is essentially same whereas it is slightly lower in $S3$ (6·31%). The minor phase of calcium sulphate hemihydrate is present in all the samples with their content as 4·48%, 1·97% and 3·62% in samples $S1$, $S2$ and $S3$, respectively. Gypsum is present only in $S1$ and $S3$ (1·17% and 1·27%, respectively) and is highly preferred oriented along 001 direction. The effect of the difference in phase composition of these samples on their hydration performance is explored by quantitative measurement of the degree of hydration of these samples as a function of time in a cement paste with w/c ratio 0·5 and is discussed in the following section. The cumulative particle size distribution data of the three samples up to 10 μm size is shown in figure 12.

5.4 *Quantitative analysis of cement hydration process*

The degree of hydration of these OPC samples was determined as a function of time, by monitoring the change in the relative intensity of C_3S peak (at $2\theta = 29\cdot42°$) with respect to rutile peak (at $2\theta = 27\cdot45°$) that was used as an internal standard with the reaction products in this work. Figure 13 shows the XRD diffractograms of hydration products of sample $S1$ as a function of time up to 72 h. The progressive decrease in the intensity of alite peak at 29·42° with reaction time is quite evident from this set of diffractograms. The relative intensity of this peak with respect to unreacted sample (0 h) was used to measure the degree of hydration (α).

Figure 14a shows the variation of the degree of hydration (α) as a function of time up to 72 h for three OPC cement samples $S1$, $S2$ and $S3$, respectively. It is quite obvious from the results that the induction period of hydration reaction for samples $S1$ and $S2$, which have similar level of C_3S content, was roughly between 3 and 4 h and the corresponding period for sample $S3$, which has about 20% less C_3S, is about 6 h. The acceleratory period continues up to 24 h for all the samples but there is substantial difference in values of degree of hydration (α) in the period 6–24 h. For example, the values of α after 12 h of hydration are 22% for $S1$, 15% for $S2$ and 8% for $S3$, respectively. The lower values of α for the sample $S3$ may be attributed primarily to the higher value of (β-C_2S/C_3S) ratio which is 0·43 for sample $S3$ compared with 0·34 and 0·32 for samples, $S1$ and $S2$, respectively. It is well known from literature that the higher value of belite to alite ratio in cement clinker reduces the rate of reaction in early stage of cement hydration (Osbeck and Jons 1980). At 24 h, α values of $S2$ and $S3$ come closer to each other. The profile of the hydration curves of the samples beyond 24 h, however, show some change in the rate of hydration for samples $S2$
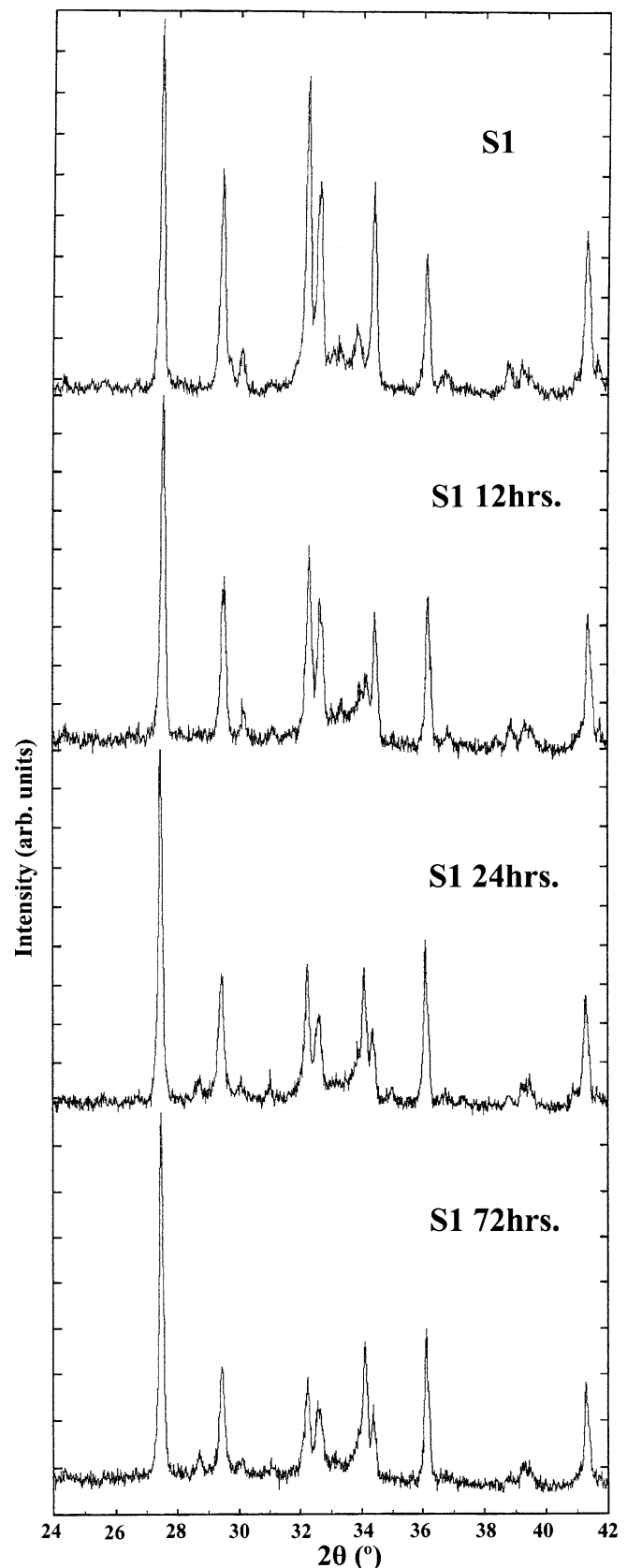

Figure 13. Experimental X-ray diffractograms of hydration products of OPC cement sample $S1$ along with rutile as a function of time.

and S3 while S1 increases monotonically. The switch-over of the hydration curves of S2 and S3 beyond 24 h of hydration may be explained from the particle size distribution of these samples.

Since the finer fraction of the particles contributes significantly towards hydration at early stage, we concentrate on the particle size distribution curves of the samples below 5 μm (figure 13). A comparison of particle size distribution curves below 5 μm show that the cumulative values at 5 μm size are quite close for samples S1 (17·9%) and S3 (18·7%) but is significantly lower for sample S2 (12·56%) and that might be one of the reasons for the higher rate of hydration for sample S3 beyond 24 h as compared to sample S2. Further, comparing the performance of samples S1 and S2, the higher degree of hydration of sample S1 may be attributed to higher percentage of finer particles present in sample S1 compared with sample S2, which is otherwise very similar to S1 in terms of phase composition ratio β-C$_2$S/C$_3$S. Although finer fraction of particle size distribution of S3 below 5 μm is slightly better compared with S1, the lower value of β-C$_2$S/C$_3$S ratio of S1 is responsible for higher values of degree of hydration of S1 beyond 24 h.

In order to analyse and interpret the comparative hydration performance of these cement samples, we have also computed the theoretical degree of hydration (α) of monodispersed spherical C$_3$S particles as a function of time for

water/C$_3$S ratio of 0·5 and particle sizes varying in the range of 2 to 7 μm based on Pommersheim–Clifton model (Pommersheim and Clifton 1979, 1982). The degree of hydration (α) of C$_3$S particles was determined from the numerical solution of (5) and (6). For numerical solution of (5), identical set of base case parameters were used in this work as was originally used by Pommersheim and Clifton (1982) in their work. The computed results of α as a function of time for different particle sizes are shown in figure 14b. The good similarity of two sets of curves is quite evident from the comparison of figures 14a and b. This similarly also indicates that the set of experimental curves of degree of cement hydration are well spanned by the set of theoretical curves of C$_3$S hydration when the particle size varies in the range of 2–7 μm leading to the conclusion that the early stage of cement hydration is primarily dominated by finer fraction of cement particles in the range of 2–7 μm. More elaborate theoretical analysis of the experimental results of OPC cement hydration process, which also includes the effect of particle size distribution of the samples, will be reported shortly.

6. Conclusions

(I) Theoretical X-ray diffractograms are very important for establishing the identity of each component of cement and its crystal phase and also its relative abundance in cement and clinker. Both qualitative and quantitative analyses are very important for a comprehensive characterization of cement and determination of phase composition of cement and clinker.

(II) Calculations of the phase composition of the OPC cement samples based on Rietveld refinement method shows more comprehensive and accurate results compared to Bogue method. All the phases present in a cement sample including the minor phases can be determined by Rietveld refinement method, whereas Bogue method provides data of cement composition based only on four major phases.

(III) The phase composition analysis of three OPC cement samples shows that samples S1 and S2 are quite similar to each other w. r. t. β-C$_2$S/C$_3$S ratio (0·34 and 0·32, respectively), but the sample S3 is quite different from S1 and S2 with a much higher value of β-C$_2$S/C$_3$S ratio (0·43). As a result of this difference in composition, the performance of sample S3 during the early stage hydration reaction is inferior compared to S1 and S2. The finer fraction of cement particles present in the samples influences significantly the degree of hydration at the early stage.

(IV) Comparison of the experimental results of the degree of hydration of OPC cement samples with theoretical degree of hydration of spherical C$_3$S particles with same water/solid ratio (0·5) indicates that the early stage hydration of the samples is dominated significantly by the cement particles in the range of 2–7 μm size.
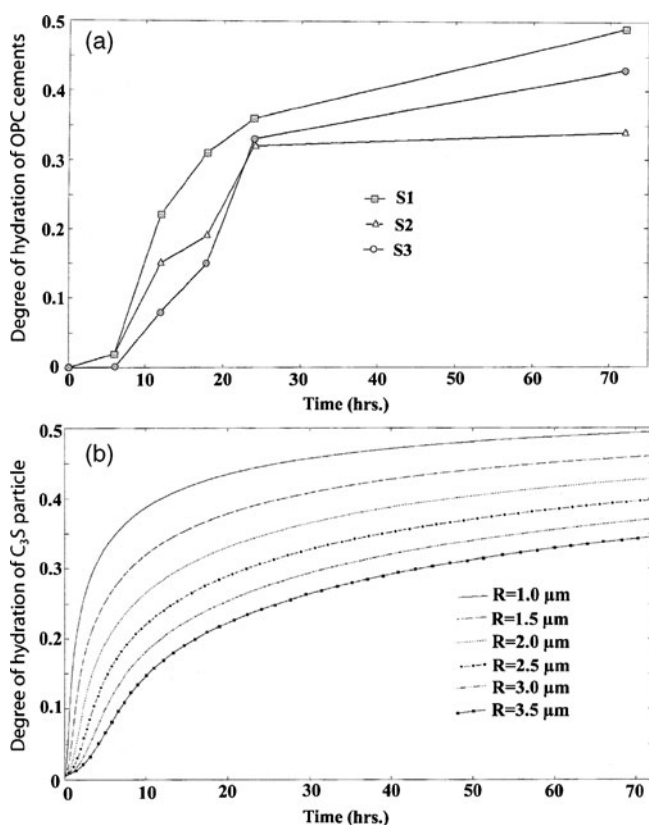

Figure 14. Comparison of experimental (**a**) and theoretical (**b**) degree of hydration.

Acknowledgements

References

Benzou C, Nonat A J and Mutin C 1995 *J. Solid State Chem.* **117** 165

Bish D L and Howard S A 1988 *J. Appl. Crystallogr.* **21** 86

Bogue R H 1955 *The chemistry of Portland cement* (New York: Reinhold Publication) 2nd ed.

Colville A A and Geller S 1971 *Acta Crystallogr.* **B27** 2311

Costa U and Marchi M 2003 *Proceedings of 11th ICCC* (Durban) p. 151

Cullity B D 1978 *Elements of X-ray diffraction* (USA: Addison-Wesley) 2nd ed.

De La Torre A G, Cabeza A, Calvente A, Bruque S and Aranda M A G 2001 *Anal. Chem.* **73** 151

De La Torre A G, Bruque S, Campo J and Aranda M A G 2002 *Cem. Concr. Res.* **32** 1347

Ferraris C F, Hackley V A and Aviles A I 2004 *Cem. Concr. Aggr.* **26** 1

Golovastikov N I, Matveeva R G and Belov N V 1975 *Sov. Phys. Crystallogr.* **20** 441

Hewlett P C (ed.) 1988 *Lea's chemistry of cement and concrete* (Oxford: Elsevier Butterworth-Heinemann) 4th ed.

Hill R J and Howard C J 1987 *J. Appl. Crystallogr.* **20** 467

Inorganic Crystal Structure Database: http://www.icsd.iqfr.csic.es/index.html

Jost K H, Ziemer B and Seydel R 1977 *Acta Crystallogr.* **B33** 1696

Mondal P and Jeffery J W 1975 *Acta Crystallogr.* **B31** 689

Mumme W G 1995 *Neues. Jahrb. Mineral. Monatsh* 145

Nishi F and Takeuchi Y 1975 *Acta Crystallogr.* **B31** 1169

Nishi F and Takeuchi Y 1984 *Z. Kristallogr.* **168** 197

Okada K and Ossaka J 1980 *Acta Crystallogr.* **B36** 919

Osbeck B and Jons E S 1980 *Proceedings of 7th ICCC* **II** II135

Peterson V K 2003 *Diffraction investigation of cement clinker and tricalcium silicate using Rietveld analysis*, PhD thesis, University of Technology, Sydney, Australia

Pommersheim J M and Clifton J R 1979 *Cem. Concr. Res.* **9** 765

Pommersheim J M and Clifton J R 1982 *Cem. Concr. Res.* **12** 765

Rodríguez-Carvajal J. Fullprof 2000 (version 4.30 Apr. 2008): http://www.ill.eu/sites/fullprof/

Rietveld H M 1969 *J. Appl. Crystallogr.* **2** 65

Schofield P F, Knight K S and Stretton I C 1996 *Am. Mineral.* **81** 847

Scrivener K L, Füllmann, T, Gallucci E, Walenta G and Bermejo E 2004 *Cem. Concr. Res.* **34** 1541

Stutzman P E 1996 Guide for X-ray powder diffraction analysis of Portland cement and clinker, NISTIR 5755

Taylor H F W 1997 *Cement chemistry* (London: Thomas Telford) 2nd ed.

Taylor J C and Hinezak I 2004 *Rietveld made easy* (Canberra, Australia: Sietronics)

Udagawa S, Urabe K, Natsume M and Yano T 1980 *Cem. Concr. Res.* **10** 139

Young R A (ed.) 1993 *The Rietveld method, IUCr monographs on crystallography-5* (New York: Oxford Science)

Young R A, Mackie P E and Von Dreele R B 1977 *J. Appl. Crystallogr.* **10** 262